

81-5-98

DEUTSCHES ELEKTRONEN-SYNCHROTRON **DESY**

DESY 81-019
April 1981

INCLUSIVE PRODUCTION OF BARYONS
IN DECAYS OF THE $T(9.46)$ AND IN QUARK JETS

by

W. Hofmann

Institut für Physik der Universität Dortmund

NOTKESTRASSE 85 · 2 HAMBURG 52

DESY behält sich alle Rechte für den Fall der Schutzrechtserteilung und für die wirtschaftliche Verwertung der in diesem Bericht enthaltenen Informationen vor.

DESY reserves all rights for commercial use of information included in this report, especially in case of apply for or grant of patents.

**To be sure that your preprints are promptly included in the
HIGH ENERGY PHYSICS INDEX ,
send them to the following address (if possible by air mail) :**

**DESY
Bibliothek
Notkestrasse 85
2 Hamburg 52
Germany**

1) Introduction

The production of mesons by quark fragmentation is fairly well described by phenomenological models¹⁾, resp. can be understood in the very intuitive picture of breaking color strings^{2,3)}, which also yields a reasonable quantitative description.^{4,5)}

More recently attempts have been made to derive meson spectra in quark- and gluon-jets from "first principles" of QCD.^{6,7)} These models assume that the initial parton initiates a cascade of partons with successively decreasing Q^2 . At a transition point Q_0^2 the partons recombine into mesons, according to a recombination mechanism^{8,9)} borrowed from the description of meson production in hadronic reactions.⁸⁾ Although the rigorous theoretical foundation of this procedure is still open, the results look promising⁶⁾.

Our present understanding of baryon production in quark or gluon jets is much worse; especially two new results from DORIS and PETRA seem surprising:

- in decays of the τ -meson, the DASP II group observed evidence for an enhancement of proton production, as compared to the nearby continuum¹⁰⁾.

- at PETRA-energies, the fraction of fast baryons among the quark fragments is as large as 10... 15%, and increases with the momentum of the secondaries.¹¹⁾

The first observation could be explained by assuming the existence of exclusive few-body decay channels of the τ -meson into final states containing a baryon pair. Due to the large mass of the τ , however, these channels are unlikely to have substantial branching ratios. Since the τ is known to decay predominantly via three gluons¹²⁾, one is tempted to consider the first observation, at least, as a hint for an increase of baryon production in gluon jets as compared to quark jets.

Inclusive Production of Baryons
in Decays of the τ (9.46)
and in Quark Jets

by

W. Hofmann

Institut für Physik
der Universität Dortmund

Abstract

Inclusive production of mesons and baryons in quark jets at $\sqrt{s} = 9.5 \dots 36$ GeV and in decays of the τ (9.46) meson has been studied using the Quark Recombination Model (QRM). The model predictions for quark jets agree with data. The QRM-simulation of three-gluon decays of the τ (9.46) shows an enhancement of the inclusive baryon rate, as was observed recently by the DASP II experiment.

In this paper, we shall describe a simple, although fairly general model for baryon production in parton fragmentation. The model, based on the quark recombination model (QRM) ⁸, accounts for the observations cited above without introducing new, and arbitrary fragmentation functions.

2) Quark Recombination Model

The idea how to explain an increase of baryon production in gluon jets (and especially in τ decays) is obvious. According to QCD, a primary parton of large Q^2 branches successively into partons of lower Q^2 , which in turn emit new partons and so on, until a mass scale is reached where confinement forces lead to quark-recombination into color-singlet hadrons. ^{13,14} At least asymptotically, the multiplicity of partons in a parton shower initiated by a primary gluon is predicted to be 9/4 as large as in quark jets ¹³. The enhanced density of partons in phase-space makes three-parton recombination more likely, and hence yields more baryons. In reactions where more than 2 hard partons are produced, like in $\tau \rightarrow ggg$, or $e^+e^- \rightarrow q\bar{q}g$, the jets may overlap with each other in phase space, resulting in a further increase of both parton density and baryon rate.

We shall first give a brief review of the "classical" QRM, which has been successfully applied to meson production in various proton induced reactions, ¹⁵ meson induced reactions ¹⁶, to two-particle correlations ^{17,19}, and to baryon production in hadronic reactions. ^{18,19}

In the framework of the QRM, the inclusive meson- and baryon-spectra in (infinite momentum!) quark or gluon jets, $q\bar{q} \rightarrow M, B+X$ or $gg \rightarrow M, B+X$, are given by

$$x D_{q,g}^M(x, Q^2) = \int \frac{dx_q}{x_q} \frac{dx_{\bar{q}}}{x_{\bar{q}}} G(x_q, x_{\bar{q}}, Q^2) R^M(x, x_q, x_{\bar{q}}) \quad (1)$$

$$x D_{q,g}^B(x, Q^2) = \int \frac{dx_q}{x_q} \frac{dx_{q'}}{x_{q'}} \frac{dx_{q''}}{x_{q''}} G(x_q, x_{q'}, x_{q''}, Q^2) R^B(x, x_q, x_{q'}, x_{q''}) \quad (2)$$

$G(x_q, x_{q'})$ is the inclusive distribution of (constituent) quarks and antiquarks of the "mass" Q_0^2 within a jet initiated by a quark or gluon of the "mass" Q^2 ; $G(x_q, x_{q'}, x_{q''})$ is the corresponding three-quark distribution. x_i denotes the usual light-cone fraction of the momentum, with respect to the primary partons momentum. In principle, G can be obtained from perturbative QCD ¹³, provided that Q_0 is larger than the QCD scale parameter Λ . As to deal with gluons generated during the evolution of the jet, it became customary to assume that close to the recombination scale Q_0 all gluons split into quark-antiquark pairs ^{6,20}. This prescription can be motivated in a sense that in the final stage of a perturbative jet there is an equilibrium between quark and gluon partons. ¹³, which is distorted once quarks start to condense into colorless objects.

Concerning the probability R^M for quark-antiquark recombination into mesons, it is assumed that two-body recombination dominates (provided that the missing mass X is well above the resonance region, allowing to neglect Regge-contributions ²²). Furthermore R^M will be proportional to the square of the meson wave function, yielding ^{8,9}

$$R^M(x, x_q, x_{q'}) \sim G^M(\xi_q, \xi_{q'}) \sim \xi_q \xi_{q'} \delta(1 - \xi_q - \xi_{q'}) \quad (3)$$

with $\xi_q = x_q/x$, and similarly ^{18,23}

$$R^B(x, x_q, x_{q'}, x_{q''}) \sim \xi_q \xi_{q'} \xi_{q''} \delta(1 - \xi_q - \xi_{q'} - \xi_{q''}) \quad (4)$$

Assuming that the effective multi-quark distribution is essentially governed by phase-space constraints, like in Kuti-Weisskopf-type models ²⁴,

$$G(x_1, x_2, \dots, x_n) \sim \kappa^n (1 - \sum_{i=1}^n x_i)^m \quad (5)$$

one finds

$$\frac{D_g^B(x)}{\left(\frac{M}{D_g}\right)} = \kappa_{jet}^{gluon} = \frac{9}{4} \kappa_{jet}^{quark} = \frac{9}{4} \frac{D_q^B(x)}{\left(\frac{M}{D_q}\right)} \quad (6)$$

Asymptotically, the relative abundance of baryons in gluon jets as compared to quark jets will be enhanced by the classical color-factor 9/4.

3) The event generator

To describe decays of the τ meson into hadrons via an intermediate three-gluon state, the QRM as defined by (1)-(6) has to be modified, since it suffers from several drawbacks:

- the recombination function R refers to partons with collinear momenta only. For the present purpose, a lorentz invariant R is required, which applies as well to slow partons with non-collinear momenta
- the QRM refers to the production of fast hadrons only . During the production of slow hadrons in regions of phase space where the parton density is large, it may happen that several antiquarks, e.g., compete with each other in trying to recombine with a given quark. This effect is not included in the standard QRM
- Monte-Carlo studies²⁵⁾ of the branching process of jet formation have demonstrated that the approach to asymptotic conditions, like (6) is extremely slow, and that at present energies the parton spectrum is dominated by phase space restrictions

In order to overcome these problems, the process of quark generation and recombination has been simulated as an exclusive

reaction in a Monte Carlo approach, thereby keeping trace of all nonasymptotic effects due to non-zero particle masses and -transverse momenta. To simulate the final confinement step, a lorentz invariant generalisation of the recombination function is proposed. By construction, the model avoids problems of double counting (which occur in the standard QRM for slow hadrons): the chance for a given quark i to recombine with another quark j is reduced, if other quarks are close to i in phase space.

The main building block of the model is a generator for exclusive n-parton densities. Such a parton cloud arises e.g. during the confinement of a quark and an antiquark moving in opposite directions.

Since QCD-calculations of the development of parton jets have proven that phase-space constraints dominate the evolution of parton densities at present energies,²⁵⁾ and since QCD formulae are expected to be rather unreliable at masses below ~ 1 GeV, a phase-space model with limited transverse momentum with respect to the axis of the initial quark has been used to describe the distribution of quarks of "size" Q_0 within a jet. The matrix element f for quark production in the parton cascade is assumed to depend only on the transverse energy E_{\perp} of the quark

$$f(p_{\perp}, p_{\perp 1}) \sim \exp(-B E_{\perp}) \quad (7)$$

Scaling of spectra in E_{\perp} is expected in QCD-based parton models^{2,3)}, the slope $B = 6.5 \text{ GeV}^{-1}$ has been chosen to fit the measured mean p_{\perp} of final state particles. In a string model of hadrons, B is related to the Regge slope α' via $B = \pi/\sqrt{2\alpha'} = 4 \text{ GeV}^{-1}$ which is not too far from the value actually used. Since quark transverse momenta are explicitly included,²⁶⁾ the rest masses of the quarks are given by their current masses ($m_u = m_d = 10 \text{ MeV}$, $m_s = 350 \text{ MeV}$). For u- and d-quarks, E_{\perp} is almost entirely given by their transverse momenta; the precise value

of $m_{u,d}$ is uncritical. The large s-quark mass however introduces a SU(3) breaking - the ratio of strange to nonstrange quarks is ≈ 0 at $P_L = 0$ and approaches $1/2$ for $P_L \gg m_s$.

Since the matrix element (7) is identical for all types of quarks, the model in its present form does not include "leading flavor" effects²⁷⁾. The flavor of the primary quark is simply assigned to an arbitrary "final state" quark. The flavors of the remaining cascade partons are chosen based on (7).

The multiplicity of generated quarks is adjusted such as to reproduce the KNO-scaling observed experimentally²⁸⁾.

In the next step, the recombination of quark-partons into mesons and baryons has to be simulated.

A Lorentz invariant formulation of the recombination cross section R can be achieved by noting that (3) describes an interaction of short range in rapidity. In other words, R is large for quark systems of low invariant mass M:

$$R^M(x, x_1, x_2) \sim \xi_1 \xi_2 \frac{m^2}{M^2} \quad (8)$$

m is the effective mass of the quark-partons. In this paper R has been chosen to

$$R \sim \exp(-M^2/2\Lambda_0^2) \quad (9)$$

inspired by the sharply cut-off mass distribution of colorless clusters in QCD jets.²⁵⁾ Λ_0 defines the effective range of confinement forces between partons. Λ_0 is expected to be of the same order as e.g. the scale parameter governing the violations of scaling observed in deep inelastic lepton-nucleon scattering (independent of its interpretation in terms of leading-order QCD graphs or non-leading higher twist effects!), the recombination scale Q_0 , or the ρ meson mass. We choose $\Lambda_0 = 0.5$ GeV. R is used for both quark-antiquark and three-quark recombination, except for an additional suppression factor 3 in the latter case,

since three arbitrary quarks have a chance of $1/27$ to be in a color singlet state, as compared to $1/9$ for a $q\bar{q}$ pair.²⁹⁾ The recombination then proceeds as follows: for a given quark i, the probabilities for recombination into mesons, W_{ij} , and into baryons, W_{ijk} , are calculated according to (9) and their sum is normalized to 1. According to these probabilities, a specific mode of recombination is chosen at random.

The spin/parity assignment of the hadron is derived via the principle of semi-local duality³⁰⁾. For example, let \bar{m}_0 and \bar{m}_1 be the mean mass of nonstrange mesons of spin 0 and spin 1, respectively. A bound $u\bar{d}$ quark system is taken to have spin 0, if $m_{u\bar{d}} < \frac{1}{2}(\bar{m}_0 + \bar{m}_1)$, and spin 1 else. Tensor meson production is neglected. Meson mixing angles are as described in ref. 1). For three-quark recombination, only the low-lying octet or decuplet baryon states were considered; the excitation of higher masses turned out to be negligible.

After deciding on the spin/parity of the hadron, its energy is corrected to put its mass on the nominal value.

At this stage, the total energy of all hadrons will differ slightly from the initial cms energy. In order to avoid any distortion of inclusive spectra, longitudinal momenta of particles are rescaled in order to ensure exact conservation of energy (if a rescaling of more than 10% is required, the event is rejected).

Finally, unstable hadrons decay.

Gluon jets, which originate e.g. from the decay of a heavy $q\bar{q}$ state into two or three gluons are simulated as follows: each gluon splits into a $q\bar{q}$ pair according to a branching function $p(x)$. A quark q from one gluon and an antiquark \bar{q}' from another gluon form a $q\bar{q}$ system whose cms moves at a speed $\hat{\beta} = (\vec{p}_q + \vec{p}_{\bar{q}'}) / (E_q + E_{\bar{q}'})$ with respect to the overall cms. This $q\bar{q}$ system is fragmented into a cloud of quarks distributed along the color-anticolor axis. Finally, the joint quark distributions from the two or three gluons are recombined into mesons or baryons.

Two types of splitting functions have been used

- a) LUND-type ²⁾ $P(x) \sim \delta(x-0.5)$
- b) QCD-type ¹³⁾ $P(x) \sim x^2 + (1-x)^2$ (10)

Note that even with the LUND fragmentation function, where each quark in the parton cascade has $x \leq 0.5$, mesons with $x > 0.5$ will be produced by recombination of quarks from different $q\bar{q}$ sub-systems.

4) Results

Fig. 1 compares the predictions of the recombination model with experimental data on quark fragmentation. ^{11,31,32)} In the model calculation for the high-energy data at $\sqrt{s} = 30 \dots 36$ GeV, the existence of $q\bar{q}g$ -events has not been taken into account explicitly. The increase of parton densities, which occurs due to the additional gluon jet, however, is implicitly contained in the model, since multiplicities are chosen such as to reproduce the experimental values.

Another approximation concerns those events with primary charmed- or bottom quarks. Since the model is not yet able to deal with decays of charmed hadrons, these events have been treated as $s\bar{s}$ events. Assuming that charmed quarks predominantly decay in the Cabibbo-favored mode, this assignment correctly accounts for the number of stable strange hadrons per event. It has been checked that this simplification does not lead to major systematic effects, at least at the present level of accuracy. The fraction of $b\bar{b}$ events is anyhow small and has been entirely neglected.

Fig. 1a) shows the inclusive spectrum of charged hadrons as a function of $x_p = P/P_{beam}$. The theoretical curves are absolutely normalized, using $R = \sigma_{had}/\sigma_{\mu\mu} = 3.8$.

Fig's 1b) and 1c) display inclusive kaon- and proton spectra. Obviously the high-energy scaling limit of the model predictions is not yet reached at DORIS energies, at least as far as production of heavy hadrons is concerned. ³³⁾

It is interesting to note that the model also predicts, via semi-local duality, a ratio of direct ρ -meson to direct π -meson production of 1.06 (averaged over x and P_T) which is close to the commonly accepted value of $\sim 1.1, 34)$

Fig. 2a) displays the model predictions for inclusive spectra of stable hadrons in quark jets, gluon jets and in three-gluon decays of the T -meson. The T -spectra are compared for the two extreme choices of the gluon splitting function (10). The mean multiplicity in T decays as compared to quark jets is predicted to increase by $14 \dots 18\%$, depending on the choice of $p(z)$. These numbers are in fair agreement with data:

EXP.	$\frac{\langle n_{ch} \rangle_T}{\langle n_{ch} \rangle_{q\bar{q}}} - 1$
PLUTO ¹²⁾	$19 \pm 3 \%$
LENA ¹²⁾	$18 \pm 5 \%$
DASP II (INCLUSIVE) ¹⁰⁾	$14 \pm 10 \%$
DASP II (FULL EVENTS) ¹²⁾	$14 \pm 4 \%$

This relatively modest increase of $\langle n_{ch} \rangle$ might seem embarrassing, since the sum of the parton multiplicities in the parton clouds generated by the three gluon jets is expected to grow much stronger. In fact, the number of quarks from the parton cascades increases by $27 \dots 35\%$. However, this increase is partly cancelled by an effect pointed out first by Brodsky ³⁵⁾: due to the increased density of partons in phase-space, the mean $q\bar{q}$ mass decreases, and the ratio of

direct ρ -mesons to direct π -mesons, e.g., reduces to ~ 0.6 . Thus the number of stable final hadrons grows slower than the number of primary hadrons.

Fig. 2b) compares predictions for the Lorentz invariant cross-sections $\tau \rightarrow ggg \rightarrow \pi^+ + X$ and $\tau \rightarrow ggg \rightarrow p, \bar{p} + X$ to recent data from DASP II¹⁰⁾. The overall agreement is satisfying, although the slopes of the spectra are predicted slightly too flat.

The model calculations show that integrated over the whole range in x , the fraction of baryons among the secondaries is augmented by 30...45% in τ decays as compared to $q\bar{q}$ jets. This enhancement of baryon production is more clearly visualized in fig. 2c) where the ratio of inclusive cross sections in quark jets and in τ decays is plotted vs. $x = 2E/\sqrt{s}$. At small x the number of baryons in τ decays is calculated to be 1.7...2.3 times as large as in $q\bar{q}$ jets, which is in qualitative agreement with the DASP II results also shown in fig. 2c). Quantitatively, the measured baryon enhancement is even larger than predicted by the model; however, once the size of the error bars is taken into account it seems premature to draw definite conclusions.

Let me finally remark that the model predicts a small decrease ($\sim 20...30\%$) of kaon yields on the τ as compared to the nearby continuum. The reason is that the increased strange particle production by gluons does not fully compensate for the absence of primary charmed quarks, which decay into strange mesons (in contrast to the other model results, this last prediction however depends strongly on the precise value of strange quark mass used in (7)).

5) Discussion

As is obvious from figs. 1) and 2) the model agrees reasonably well with data, especially as far as proton production in quark jets and in τ -decays is concerned.

At this point, it should be mentioned that it has not been tried to vary parameters in order to obtain a perfect fit to the data points; the only quantities adjusted to match the data on quark jets are the multiplicity distribution for charged secondaries and the mean p_T of secondaries.

To judge the physical significance of the results shown above one has to know how stable the model is with respect to changes in the various assumptions put in. During the development of the model, a number of different versions were used: in a first attempt, two- and three-parton recombination was studied for identical partons, ignoring flavor effects and resonance production; the next step was to consider the SU(3) breaking due to the different quark masses, and finally resonance production was included. Besides the phase-space event generator, a recursive generator simulating the successive breaking of color strings (like in the LUND-model²⁾) and a QCD-like branching process¹³⁾ were employed. In addition, different parametrizations of the recombination function R were tried. All these models yielded very similar results for the inclusive spectra once the multiplicity distribution was correctly adjusted; all show an enhancement of baryon production in τ -decays by factors up to 3, and all predict a substantial fraction of large-momentum protons in quark jets.

Furthermore, the main results presented in this paper are expected to hold for the whole class of models which are based on a similar physics as the QRM. Such models are e.g. the valon picture⁶⁾, or the QCD jet calculus leading to a preconfinement stage.^{13,25)}

Although the model has been developed with the aim to understand the enhancement of baryon production in τ -decays, it can be applied to other deep inelastic reactions as well. The two following predictions e.g. allow to check the basic assumptions used in the model:

- in the reaction $e^+e^- \rightarrow q\bar{q}g$, the ratio of baryon to meson cross sections rises in that hemisphere of the event which contains a quark and the gluon ("fat jet"-side), as compared to the opposite hemisphere ("slim jet")
- in hadronic interactions, where particles or jets of large transverse momentum (with respect to beam axis) are produced, the fraction of slow antiprotons should increase as compared to "normal" inelastic hadronic interactions, since in the central region of such events four parton jets (the two jets of large p_T and two spectator jets) overlap.

Acknowledgement

I would like to thank Prof. D. Wegener and Dr. A. Markees for discussions and valuable comments.

This work was supported by the Deutsche Bundesministerium für Forschung und Technologie.

References

- 1) R.D. Field, R.P. Feynman, Nucl. Phys. B136 (1978) 1
- 2) B. Andersson, G. Gustafson, C. Peterson, Z.Phys. C1 (1979) 105, C3 (1980) 223, T. Sjöstrand, LU-TP-80-3 (1980)
- 3) A. Casher, H. Neuberger, S. Nussinov, Phys. Rev. D20 (1979) 179
- 4) B. Andersson, G. Gustafson, T. Sjöstrand, Z. Phys. C6 (1980) 235
- 5) JADE-Collaboration, W. Bartel et al., DESY 81/OO9 (1981)
- 6) V. Chang, R.C. Hwa, Phys. Rev. Lett. 44 (1980) 139; Phys. Rev. D23 (1981) 728
- 7) L.M. Jones et al., Phys. Rev. D23 (1981) 717
- 8) K.P. Das, R.C. Hwa, Phys. Lett. B68 (1977) 459
- 9) E. Takasugi et al., Phys. Rev. D20 (1979) 211
- 10) DASP-II Collaboration, H. Albrecht et al., DESY 81/O11 (1981)
- 11) TASSO-Collaboration, R. Brandelik et al., Phys. Lett. 89B (1980) 418; 94B (1980) 91; 94B (1980) 444
- 12) DASP II Collaboration, W. Schmidt-Parzefall, Proc. of the 19th Int. Conf. on High Energy Physics (Tokyo 1978), LENA Collaboration, F.H. Heimlich et al., Phys. Lett. B86 (1979) 399, DESY 81/OO8 (1981)
- 13) PLUTO Collaboration, G. Alexander et al., DESY 80/117 (1980)
- 14) K. Konishi, A. Ukawa, G. Veneziano, Phys. Lett. B78 (1978) 243
- 15) D. Amati, G. Veneziano, Phys. Lett. B83 (1979) 87
- 16) L. Caneschi, A. Schwimmer, Phys. Lett. B86 (1979) 179
- 17) e.g. D.W. Duke, F.E. Taylor, Phys. Rev. D17 (1978) 1788
- 18) W. Aitkenhead et al., Phys. Rev. Lett. 45 (1980) 157
- 19) E. Takasugi, X. Tata, Phys. Rev. D21 (1980) 1838
- 20) R. Migneron, J.L. Robinson, FNAL-Pub-80/72 THY (1980)
- 21) J. Ranft, Phys. Rev. D18 (1978) 1491
- 22) E. Takasugi, Proc. of the XI Int. Symp. on Multiparticle Dynamics (Bruges, 1980) p.141
- 23) V. Černý, P. Lichard, J. Pisut, Phys. Rev. D16 (1977) 2822, D18 (1978) 2409
- 24) V. Černý et al., Phys. Rev. D18 (1978) 4052
- 25) J.M. Teper, Rutherford preprint, RL-78-O22 (1978)
- 26) T.A. De Grand, Phys. Rev. D19 (1979) 1398
- 27) J.F. Gunion, Phys. Rev. D12 (1975) 3469
- 28) S.J. Brodsky, P.Lepage, SLAC-PUB-2478 (1980)
- 29) J. Kuti, V. Weisskopf, Phys. Rev. D4 (1971) 3418

Figure captions

- 25) P. Mazzanti, R. Odorico, Phys. Lett. 95B (1980) 133
 R. Odorico, Nucl. Phys. B172 (1980) 157
 G.C. Fox, S. Wolfram, Nucl. Phys. B168 (1980) 285
- 26) see e.g. F.E. Close, An Introduction to Quarks and Partons, Academic Press, London 1979. The u,d- and s-quark masses used here correspond to effective constituent-quark masses of ~ 300 and ~ 500 MeV, respectively.
- 27) TASSO-Collaboration, R. Brandelik et al., DESY 81/005 (1981)
- 28) PLUTO-Collaboration, Ch. Berger et al., Phys.Lett.95B (1980) 313
- 29) In their chromoelectric-flux-tube model of jets, the authors of ref. 3 get slightly higher suppression factors
- 30) H. Fritzsch, Phys. Lett. 67B (1977) 217
 M. Glück, J.F. Owens, E. Reya, Phys. Rev. D17 (1978) 2324
 M. Glück, E. Reya, Phys. Lett. 79B (1978) 453
- 31) DASP-Collaboration, R. Brandelik et al., Nucl. Phys. B148 (1979) 189
- 32) G.J. Feldmann, M.L. Perl, Phys. Rep. 33 (1977) 285
- 33) D. Pandoulas, Talk given at the XXth Int. Conf. on High Energy Physics, Wisconsin (1980)
- 34) see also: W. Hofmann, Jets of Hadrons, Springer Tracts in Modern Physics, in print
- 35) A ratio ρ/π of ≈ 1 is observed e.g. in large- p_T parton jets produced in pp-interactions:
 D. Drijard et al., CERN-EP 81/12 (1981)
 D. Darriulat et al., Nucl. Phys. B107 (1976) 429
- 35) S.J. Brodsky, Physica Scripta 19 (1979) 65

Fig. 1 Comparison between measured inclusive quark fragmentation spectra^{11,31,32} and model predictions

- a) $e^+e^- \rightarrow h^+ + X$
 b) $e^+e^- \rightarrow K^+ + X$
 c) $e^+e^- \rightarrow p, \bar{p} + X$

Reflecting the systematical errors of $R = \sigma_{had}/\sigma_{\mu\mu}$, the overall normalisation of model predictions vs. data is uncertain by $\pm 15\%$.

Fig. 2

- a) Inclusive particle spectra $(1/\sigma)(d\sigma/dx)$ as predicted for quark jets (—), gluon jets using $p(x) \sim x^2(1-x)^2$ (---) and τ decays into three gluons, with $p(x) \sim x^2 + (1-x)^2$ (.....) and with $p(x) \sim \delta(x-0.5)$ (---), for $\sqrt{s} = 9.46$ GeV. The shaded region indicates the range of predictions for τ -decays, depending on the specific choice of $p(x)$.
- b) Model predictions for inclusive pion (—) and proton (---) spectra in three-gluon decays of the τ as compared to data¹⁰. The curves shown refer to $p(x) \sim \delta(x-0.5)$; however for the range in x used here, the predictions do not depend strongly on $p(x)$.

Overall normalisation error $\approx \pm 20\%$.

- c) Range of model predictions for the ratio of inclusive spectra in τ decays and in quark jets, for $e^+e^- \rightarrow \pi^+ + X$ and $e^+e^- \rightarrow p, \bar{p} + X$, at $\sqrt{s} = 9.46$ GeV, compared to data¹⁰.

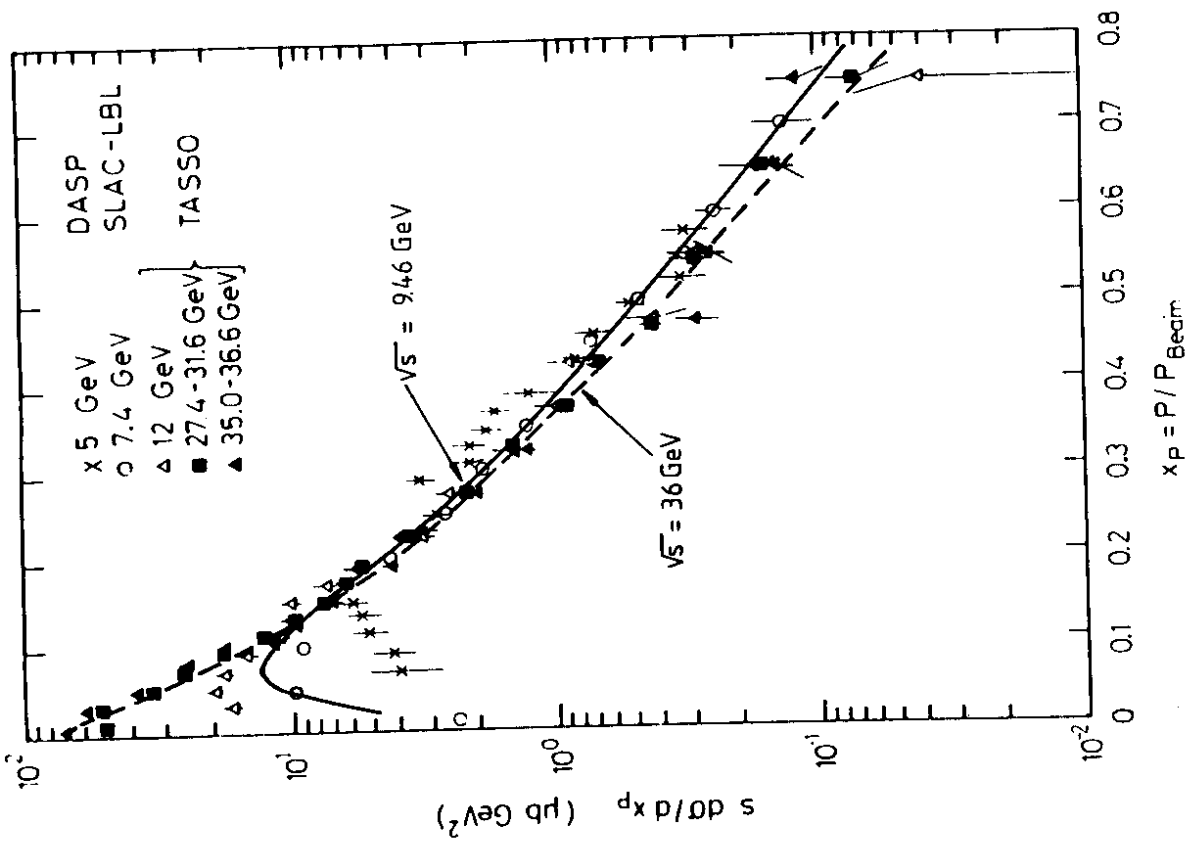


Fig. 1a)

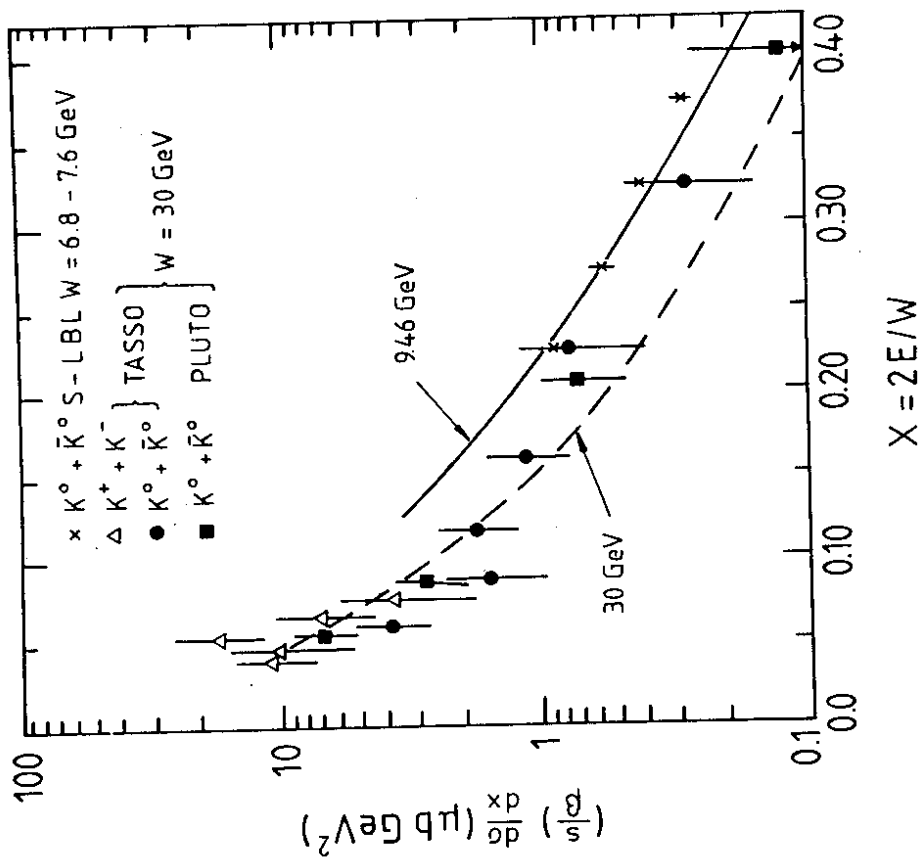


FIG. 1b

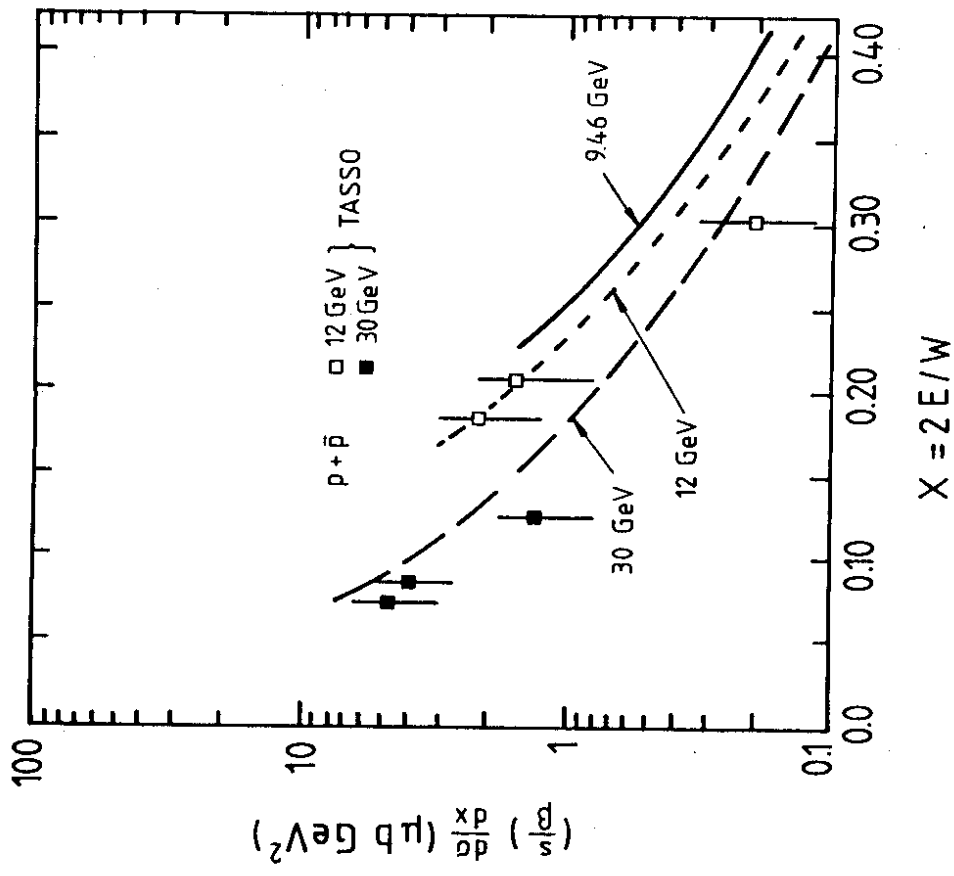


Fig. 1c)

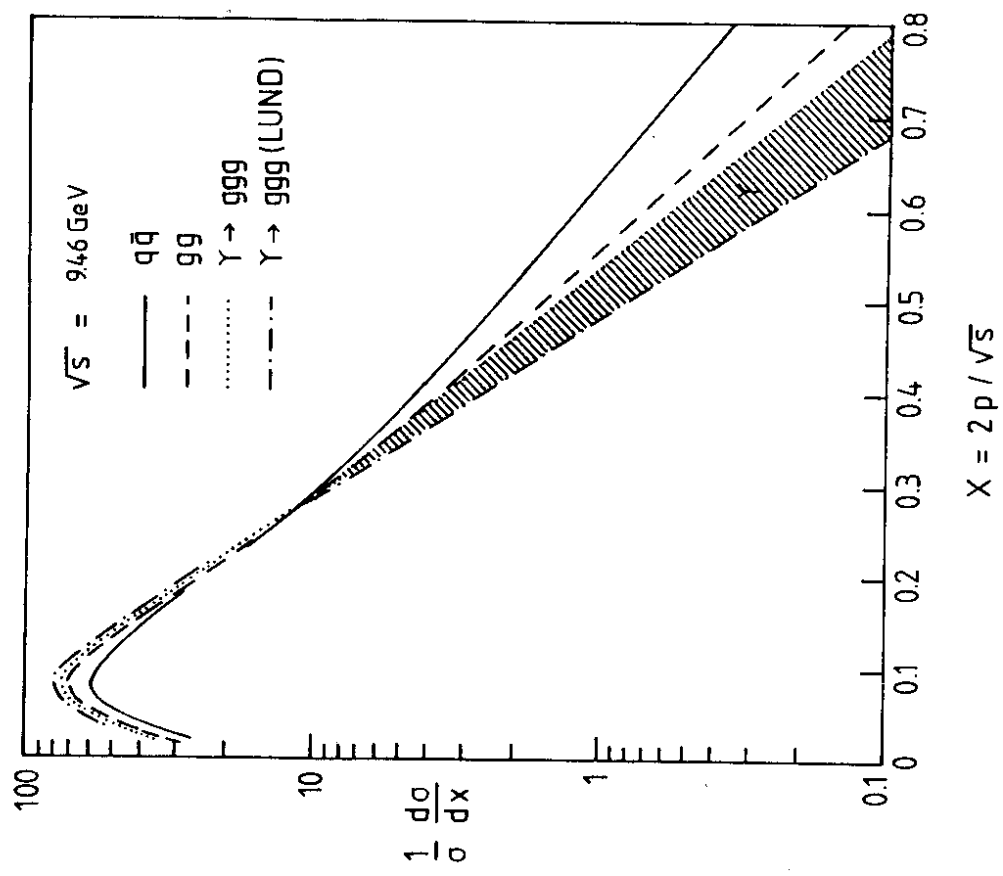


FIG.2a

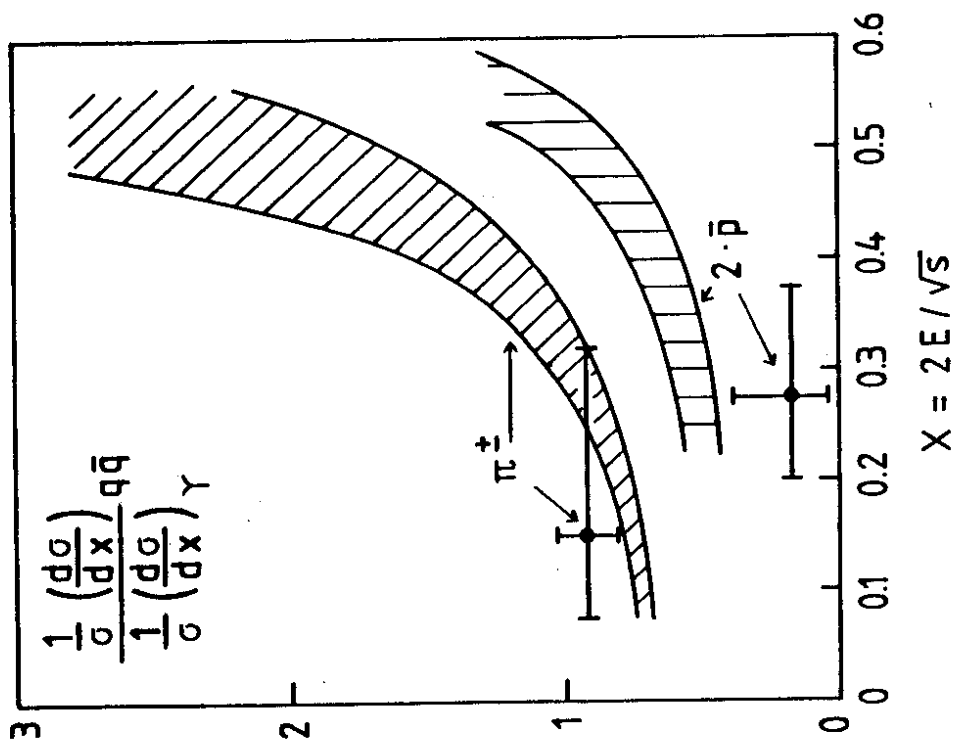
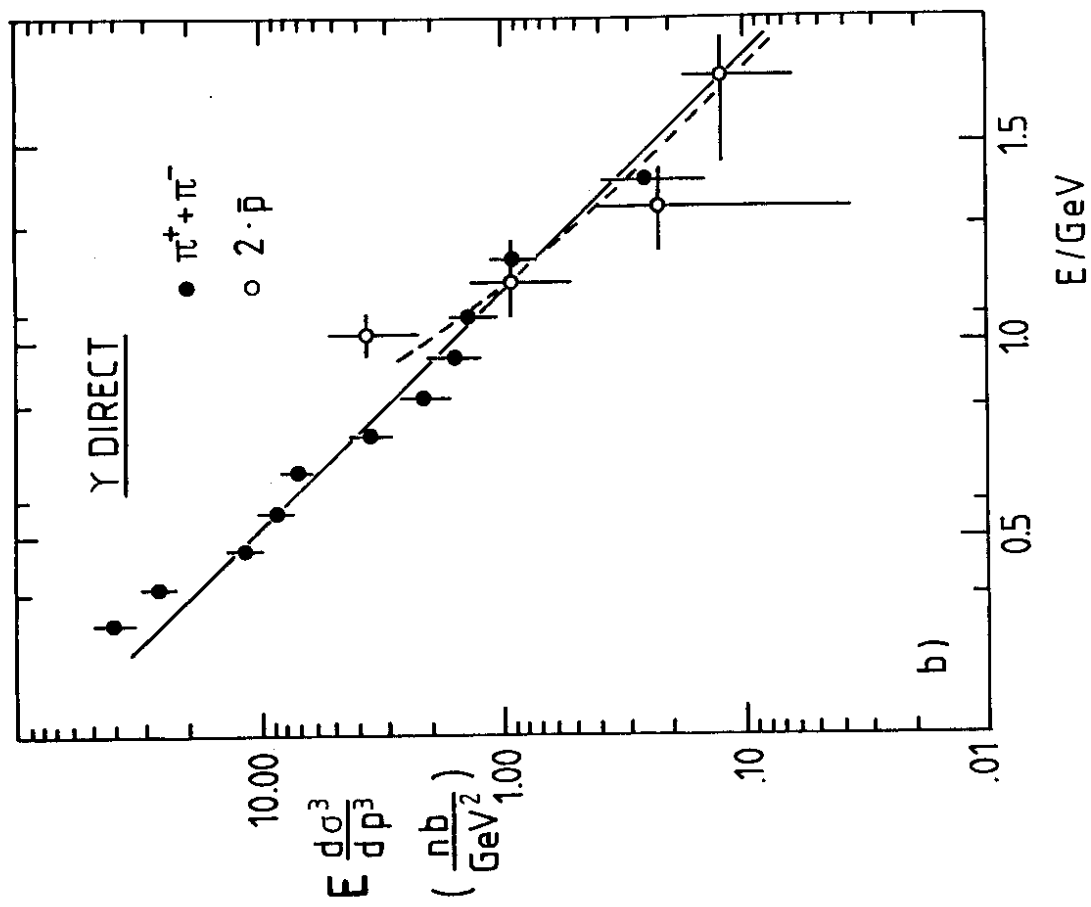


Fig. 2a)

Fig. 2b)

